

Measurement of Three-jet Distributions in Photoproduction at HERA

ZEUS Collaboration

Abstract

The cross section for the photoproduction of events containing three jets with a three-jet invariant mass of $M_{3J} > 50$ GeV has been measured with the ZEUS detector at HERA. The three-jet angular distributions are inconsistent with a uniform population of the available phase space but are well described by parton shower models and $\mathcal{O}(\alpha_s^2)$ pQCD calculations. Comparisons with the parton shower model indicate a strong contribution from initial state radiation as well as a sensitivity to the effects of colour coherence.

The ZEUS Collaboration

J. Breitweg, S. Chekanov, M. Derrick, D. Krakauer, S. Magill, B. Musgrave, J. Repond,
R. Stanek, R. Yoshida

Argonne National Laboratory, Argonne, IL, USA ^p

M.C.K. Mattingly

Andrews University, Berrien Springs, MI, USA

G. Abbiendi, F. Anselmo, P. Antonioli, G. Bari, M. Basile, L. Bellagamba, D. Boscherini,
A. Bruni, G. Bruni, G. Cara Romeo, G. Castellini¹, L. Cifarelli², F. Cindolo, A. Contin,
N. Coppola, M. Corradi, S. De Pasquale, P. Giusti, G. Iacobucci, G. Laurenti, G. Levi,
A. Margotti, T. Massam, R. Nania, F. Palmonari, A. Pesci, A. Polini, G. Sartorelli,
Y. Zamora Garcia³, A. Zichichi

University and INFN Bologna, Bologna, Italy ^f

C. Amelung, A. Bornheim, I. Brock, K. Coböken, J. Crittenden, R. Deffner, M. Eckert,
M. Grothe⁴, H. Hartmann, K. Heinloth, L. Heinz, E. Hilger, H.-P. Jakob, A. Kappes,
U.F. Katz, R. Kerger, E. Paul, M. Pfeiffer, H. Schnurbusch, A. Weber, H. Wieber

Physikalisches Institut der Universität Bonn, Bonn, Germany ^c

D.S. Bailey, O. Barret, W.N. Cottingham, B. Foster, R. Hall-Wilton, G.P. Heath,
H.F. Heath, J.D. McFall, D. Piccioni, J. Scott, R.J. Tapper

H.H. Wills Physics Laboratory, University of Bristol, Bristol, U.K. ^o

M. Capua, A. Mastroberardino, M. Schioppa, G. Susinno

Calabria University, Physics Dept. and INFN, Cosenza, Italy ^f

H.Y. Jeoung, J.Y. Kim, J.H. Lee, I.T. Lim, K.J. Ma, M.Y. Pac⁵

Chonnam National University, Kwangju, Korea ^h

A. Caldwell⁶, N. Cartiglia, Z. Jing, W. Liu, B. Mellado, J.A. Parsons, S. Ritz⁷, R. Sacchi,
S. Sampson, F. Sciulli, Q. Zhu

Columbia University, Nevis Labs., Irvington on Hudson, N.Y., USA ^q

P. Borzemski, J. Chwastowski, A. Eskreys, J. Figiel, K. Klimek, M.B. Przybycień, L. Zawiejski

Inst. of Nuclear Physics, Cracow, Poland ^j

L. Adamczyk⁸, B. Bednarek, K. Jeleń, D. Kisielewska, A.M. Kowal, T. Kowalski,
M. Przybycień,

E. Rulikowska-Zarębska, L. Suszycki, J. Zając

*Faculty of Physics and Nuclear Techniques, Academy of Mining and Metallurgy, Cracow,
Poland ^j*

Z. Duliński, A. Kotański

Jagellonian Univ., Dept. of Physics, Cracow, Poland ^k

L.A.T. Bauerdick, U. Behrens, H. Beier⁹, J.K. Bienlein, C. Burgard, K. Desler, G. Drews,
U. Fricke, F. Goebel, P. Göttlicher, R. Graciani, T. Haas, W. Hain, G.F. Hartner,
D. Hasell¹⁰, K. Hebbel, K.F. Johnson¹¹, M. Kasemann¹², W. Koch, U. Kötz, H. Kowal-
ski, L. Lindemann, B. Löhr, M. Martínez, J. Milewski¹³, M. Milite, T. Monteiro¹⁴,
D. Notz, A. Pellegrino, F. Pelucchi, K. Piotrkowski, M. Rohde, J. Roldán¹⁵, J.J. Ryan¹⁶,
P.R.B. Saull, A.A. Savin, U. Schneekloth, O. Schwarzer, F. Selonke, M. Sievers, S. Ston-
jek, B. Surov¹⁴, E. Tassi, D. Westphal¹⁷, G. Wolf, U. Wollmer, C. Youngman, W. Zeuner

Deutsches Elektronen-Synchrotron DESY, Hamburg, Germany

B.D. Burow¹⁸, C. Coldewey, H.J. Grabosch, A. Lopez-Duran Viani, A. Meyer, K. Mönig,
 S. Schlenstedt, P.B. Straub
DESY-IFH Zeuthen, Zeuthen, Germany
 G. Barbagli, E. Gallo, P. Pelfer
University and INFN, Florence, Italy^f
 G. Maccarrone, L. Votano
INFN, Laboratori Nazionali di Frascati, Frascati, Italy^f
 A. Bamberger, S. Eisenhardt, P. Markun, H. Raach, S. Wölffe
Fakultät für Physik der Universität Freiburg i.Br., Freiburg i.Br., Germany^c
 N.H. Brook, P.J. Bussey, A.T. Doyle¹⁹, S.W. Lee, N. Macdonald, G.J. McCance, D.H. Saxon,
 L.E. Sinclair, I.O. Skillicorn, E. Strickland, R. Waugh
Dept. of Physics and Astronomy, University of Glasgow, Glasgow, U.K.^o
 I. Bohnet, N. Gendner, U. Holm, A. Meyer-Larsen, H. Salehi, K. Wick
Hamburg University, I. Institute of Exp. Physics, Hamburg, Germany^c
 A. Garfagnini, I. Gialas²⁰, L.K. Gladilin²¹, D. Kçira²², R. Klanner, E. Lohrmann,
 G. Poelz, F. Zetsche
Hamburg University, II. Institute of Exp. Physics, Hamburg, Germany^c
 T.C. Bacon, J.E. Cole, G. Howell, L. Lamberti²³, K.R. Long, D.B. Miller, A. Priniias²⁴,
 J.K. Sedgbeer, D. Sideris, A.D. Tapper, R. Walker
Imperial College London, High Energy Nuclear Physics Group, London, U.K.^o
 U. Mallik, S.M. Wang
University of Iowa, Physics and Astronomy Dept., Iowa City, USA^p
 P. Cloth, D. Filges
Forschungszentrum Jülich, Institut für Kernphysik, Jülich, Germany
 T. Ishii, M. Kuze, I. Suzuki²⁵, K. Tokushuku²⁶, S. Yamada, K. Yamauchi, Y. Yamazaki
Institute of Particle and Nuclear Studies, KEK, Tsukuba, Japan^q
 S.H. Ahn, S.H. An, S.J. Hong, S.B. Lee, S.W. Nam²⁷, S.K. Park
Korea University, Seoul, Korea^h
 H. Lim, I.H. Park, D. Son
Kyungpook National University, Taegu, Korea^h
 F. Barreiro, J.P. Fernández, G. García, C. Glasman²⁸, J.M. Hernández²⁹, L. Labarga,
 J. del Peso, J. Puga, I. Redondo³⁰, J. Terrón
*Univer. Autónoma Madrid, Depto de Física Teórica, Madrid, Spain*ⁿ
 F. Corriveau, D.S. Hanna, J. Hartmann³¹, W.N. Murray¹⁶, A. Ochs, S. Padhi, C. Pin-
 ciuc, M. Riveline, D.G. Stairs, M. St-Laurent
McGill University, Dept. of Physics, Montréal, Québec, Canada^{a, b}
 T. Tsurugai
Meiji Gakuin University, Faculty of General Education, Yokohama, Japan
 V. Bashkurov, B.A. Dolgoshein, A. Stifutkin
Moscow Engineering Physics Institute, Moscow, Russia^l
 G.L. Bashindzhagyan, P.F. Ermolov, Yu.A. Golubkov, L.A. Khein, N.A. Korotkova,
 I.A. Korzhavina, V.A. Kuzmin, O.Yu. Lukina, A.S. Proskuryakov, L.M. Shcheglova³²,
 A.N. Solomin³², S.A. Zotkin
Moscow State University, Institute of Nuclear Physics, Moscow, Russia^m

C. Bokel, M. Botje, N. Brümmer, J. Engelen, E. Koffeman, P. Kooijman, A. van Sighem, H. Tiecke, N. Tuning, W. Verkerke, J. Vosseveld, L. Wiggers, E. de Wolf
*NIKHEF and University of Amsterdam, Amsterdam, Netherlands*ⁱ

D. Acosta³³, B. Bylsma, L.S. Durkin, J. Gilmore, C.M. Ginsburg, C.L. Kim, T.Y. Ling, P. Nylander
Ohio State University, Physics Department, Columbus, Ohio, USA^p

H.E. Blaikley, R.J. Cashmore, A.M. Cooper-Sarkar, R.C.E. Devenish, J.K. Edmonds, J. Große-Knetter³⁴, N. Harnew, T. Matsushita, V.A. Noyes³⁵, A. Quadt, O. Ruske, M.R. Sutton, R. Walczak, D.S. Waters
Department of Physics, University of Oxford, Oxford, U.K.^o

A. Bertolin, R. Brugnera, R. Carlin, F. Dal Corso, U. Dosselli, S. Limentani, M. Morandin, M. Posocco, L. Stanco, R. Stroili, C. Voci
Dipartimento di Fisica dell' Università and INFN, Padova, Italy^f

L. Iannotti³⁶, B.Y. Oh, J.R. Okrasinski, W.S. Toothacker, J.J. Whitmore
Pennsylvania State University, Dept. of Physics, University Park, PA, USA^q

Y. Iga
Polytechnic University, Sagamihara, Japan^g

G. D'Agostini, G. Marini, A. Nigro, M. Raso
Dipartimento di Fisica, Univ. 'La Sapienza' and INFN, Rome, Italy^f

C. Cormack, J.C. Hart, N.A. McCubbin, T.P. Shah
Rutherford Appleton Laboratory, Chilton, Didcot, Oxon, U.K.^o

D. Epperson, C. Heusch, H.F.-W. Sadrozinski, A. Seiden, R. Wichmann, D.C. Williams
University of California, Santa Cruz, CA, USA^p

N. Pavel
Fachbereich Physik der Universität-Gesamthochschule Siegen, Germany^c

H. Abramowicz³⁷, G. Briskin³⁸, S. Dagan³⁹, S. Kananov³⁹, A. Levy³⁹
Raymond and Beverly Sackler Faculty of Exact Sciences, School of Physics, Tel-Aviv University, Tel-Aviv, Israel^e

T. Abe, T. Fusayasu, M. Inuzuka, K. Nagano, K. Umemori, T. Yamashita
Department of Physics, University of Tokyo, Tokyo, Japan^g

R. Hamatsu, T. Hirose, K. Homma⁴⁰, S. Kitamura⁴¹, T. Nishimura
Tokyo Metropolitan University, Dept. of Physics, Tokyo, Japan^g

M. Arneodo, R. Cirio, M. Costa, M.I. Ferrero, S. Maselli, V. Monaco, C. Peroni, M.C. Petrucci, M. Ruspa, A. Solano, A. Staiano
Università di Torino, Dipartimento di Fisica Sperimentale and INFN, Torino, Italy^f

M. Dardo
II Faculty of Sciences, Torino University and INFN - Alessandria, Italy^f

D.C. Bailey, C.-P. Fagerstroem, R. Galea, T. Koop, G.M. Levman, J.F. Martin, R.S. Orr, S. Polenz, A. Sabetfakhri, D. Simmons
University of Toronto, Dept. of Physics, Toronto, Ont., Canada^a

J.M. Butterworth, C.D. Catterall, M.E. Hayes, E.A. Heaphy, T.W. Jones, J.B. Lane, M. Wing
University College London, Physics and Astronomy Dept., London, U.K.^o

J. Ciborowski, G. Grzelak⁴², R.J. Nowak, J.M. Pawlak, R. Pawlak, B. Smalska, T. Tymieniecka,

A.K. Wróblewski, J.A. Zakrzewski, A.F. Żarnecki

Warsaw University, Institute of Experimental Physics, Warsaw, Poland^j

M. Adamus, T. Gadaj

Institute for Nuclear Studies, Warsaw, Poland^j

O. Deppe, Y. Eisenberg³⁹, D. Hochman, U. Karshon³⁹

Weizmann Institute, Department of Particle Physics, Rehovot, Israel^d

W.F. Badgett, D. Chapin, R. Cross, C. Foudas, S. Mattingly, D.D. Reeder, W.H. Smith,

A. Vaiciulis, T. Wildschek, M. Wodarczyk

University of Wisconsin, Dept. of Physics, Madison, WI, USA^p

A. Deshpande, S. Dhawan, V.W. Hughes

Yale University, Department of Physics, New Haven, CT, USA^p

S. Bhadra, W.R. Frisken, M. Khakzad, S. Menary, W.B. Schmidke

York University, Dept. of Physics, North York, Ont., Canada^a

1 also at IROE Florence, Italy
2 now at Univ. of Salerno and INFN Napoli, Italy
3 supported by Worldlab, Lausanne, Switzerland
4 now at University of California, Santa Cruz, USA
5 now at Dongshin University, Naju, Korea
6 also at DESY
7 Alfred P. Sloan Foundation Fellow
8 supported by the Polish State Committee for Scientific Research, grant No. 2P03B14912
9 now at Innosoft, Munich, Germany
10 now at Massachusetts Institute of Technology, Cambridge, MA, USA
11 visitor from Florida State University
12 now at Fermilab, Batavia, IL, USA
13 now at ATM, Warsaw, Poland
14 now at CERN
15 now at IFIC, Valencia, Spain
16 now a self-employed consultant
17 now at Bayer A.G., Leverkusen, Germany
18 now an independent researcher in computing
19 also at DESY and Alexander von Humboldt Fellow at University of Hamburg
20 visitor of Univ. of Crete, Greece, partially supported by DAAD, Bonn - Kz. A/98/16764
21 on leave from MSU, supported by the GIF, contract I-0444-176.07/95
22 supported by DAAD, Bonn - Kz. A/98/12712
23 supported by an EC fellowship
24 PPARC Post-doctoral fellow
25 now at Osaka Univ., Osaka, Japan
26 also at University of Tokyo
27 now at Wayne State University, Detroit
28 supported by an EC fellowship number ERBFMBICT 972523
29 now at HERA-B/DESY supported by an EC fellowship No.ERBFMBICT 982981
30 supported by the Comunidad Autonoma de Madrid
31 now at debis Systemhaus, Bonn, Germany
32 partially supported by the Foundation for German-Russian Collaboration DFG-RFBR
(grant no. 436 RUS 113/248/3 and no. 436 RUS 113/248/2)
33 now at University of Florida, Gainesville, FL, USA
34 supported by the Feodor Lynen Program of the Alexander von Humboldt foundation
35 Glasstone Fellow
36 partly supported by Tel Aviv University
37 an Alexander von Humboldt Fellow at University of Hamburg
38 now at Brown University, Providence, RI, USA
39 supported by a MINERVA Fellowship
40 now at ICEPP, Univ. of Tokyo, Tokyo, Japan
41 present address: Tokyo Metropolitan University of Health Sciences, Tokyo 116-8551,
Japan
42 supported by the Polish State Committee for Scientific Research, grant No. 2P03B09308

- a* supported by the Natural Sciences and Engineering Research Council of Canada (NSERC)
- b* supported by the FCAR of Québec, Canada
- c* supported by the German Federal Ministry for Education and Science, Research and Technology (BMBF), under contract numbers 057BN19P, 057FR19P, 057HH19P, 057HH29P, 057SI75I
- d* supported by the MINERVA Gesellschaft für Forschung GmbH, the German Israeli Foundation, and by the Israel Ministry of Science
- e* supported by the German-Israeli Foundation, the Israel Science Foundation, the U.S.-Israel Binational Science Foundation, and by the Israel Ministry of Science
- f* supported by the Italian National Institute for Nuclear Physics (INFN)
- g* supported by the Japanese Ministry of Education, Science and Culture (the Monbusho) and its grants for Scientific Research
- h* supported by the Korean Ministry of Education and Korea Science and Engineering Foundation
- i* supported by the Netherlands Foundation for Research on Matter (FOM)
- j* supported by the Polish State Committee for Scientific Research, grant No. 115/E-343/SPUB/P03/002/97, 2P03B10512, 2P03B10612, 2P03B14212, 2P03B10412, 2P03B05315
- k* supported by the Polish State Committee for Scientific Research (grant No. 2P03B08614) and Foundation for Polish-German Collaboration
- l* partially supported by the German Federal Ministry for Education and Science, Research and Technology (BMBF)
- m* supported by the Fund for Fundamental Research of Russian Ministry for Science and Education and by the German Federal Ministry for Education and Science, Research and Technology (BMBF)
- n* supported by the Spanish Ministry of Education and Science through funds provided by CICYT
- o* supported by the Particle Physics and Astronomy Research Council
- p* supported by the US Department of Energy
- q* supported by the US National Science Foundation

1 Introduction

Calculations of photoproduction processes beyond leading order in perturbative QCD (pQCD) predict a rich variety of phenomena. Some of these can be studied in final states containing more than two jets. Also, the study of multijet production provides sensitive tests of extensions to fixed order theories such as parton shower models. The properties of multijet events in hadronic collisions have been the subject of earlier studies [1, 2, 3]. Dijet photoproduction accompanied by a third, low transverse energy cluster has been studied by ZEUS [4]. In this paper, cross sections and angular distributions for three or more moderately high transverse energy jets in photoproduction are presented for the first time.

Apart from the azimuthal orientation, a system of two massless jets can be completely specified in its centre-of-mass (CM) frame by the two-jet invariant mass, M_{2J} and $\cos \vartheta^*$, where ϑ^* is the angle between the jet axis and the beam-line. The distribution in $\cos \vartheta^*$ for photoproduction of dijets is forward-backward peaked with sensitivity to the spin of the exchanged fermion or boson [5].

A set of observables describing events with an arbitrary number of jets has been proposed which spans the multijet parameter space, facilitates the interpretation of the data within pQCD and reduces to M_{2J} and $\cos \vartheta^*$ for the dijet case [6]. For three massless jets there are five parameters which are defined in terms of the energies, E_i , and momentum three-vectors, \vec{p}_i , of the jets in the three-jet CM frame and \vec{p}_B , the beam direction.¹ The jets are numbered, 3, 4 and 5 in order of decreasing energy as illustrated in the schematic drawing, Fig. 1. The parameters are: the three-jet invariant mass, M_{3J} ; the energy-sharing quantities X_3 and X_4 ,

$$X_i \equiv \frac{2E_i}{M_{3J}}; \quad (1)$$

the cosine of the scattering angle of the highest energy jet with respect to the beam,

$$\cos \vartheta_3 \equiv \frac{\vec{p}_B \cdot \vec{p}_3}{|\vec{p}_B| |\vec{p}_3|}; \quad (2)$$

and ψ_3 , the angle between the plane containing the highest energy jet and the beam and the plane containing the three jets. The latter is defined by

$$\cos \psi_3 \equiv \frac{(\vec{p}_3 \times \vec{p}_B) \cdot (\vec{p}_4 \times \vec{p}_5)}{|\vec{p}_3 \times \vec{p}_B| |\vec{p}_4 \times \vec{p}_5|}. \quad (3)$$

The definition of the angles ϑ_3 and ψ_3 is illustrated in Fig. 1. Since ϑ_3 involves only the highest energy jet, the distribution of $\cos \vartheta_3$ in three-jet processes may be expected to follow closely the distribution of $\cos \vartheta^*$ in dijet events. The ψ_3 angle, on the other hand, reflects the orientation of the lowest energy jet. In the case where this jet arises from initial-state radiation, the coherence property of QCD will tend to orient the third jet close to the incoming proton or photon direction. The two planes shown in Fig. 1 will therefore tend to coincide leading to a ψ_3 distribution which peaks toward 0 and π .

¹We take the nominal beam direction as $\vec{p}_B = \hat{z}$. In the ZEUS coordinate system the z -axis is defined to be in the proton beam direction. Polar angles, ϑ , are measured with respect to the z -axis and pseudorapidity is defined as $\eta = -\ln(\tan \frac{\vartheta}{2})$.

This paper presents the three-jet inclusive cross section in photoproduction and the distribution of the three-jet events with respect to M_{3J} , X_3 , X_4 , $\cos\vartheta_3$ and ψ_3 . This work was performed with the ZEUS detector using 16 pb^{-1} of data delivered by HERA in 1995 and 1996.

2 Experimental Conditions

In this period HERA operated with protons of energy $E_p = 820\text{ GeV}$ and positrons of energy $E_e = 27.5\text{ GeV}$. The ZEUS detector is described in detail in [7, 8]. The main components used in the present analysis are the central tracking system positioned in a 1.43 T solenoidal magnetic field and the uranium-scintillator sampling calorimeter (CAL). The tracking system was used to establish an interaction vertex. Energy deposits in the CAL were used in the jet finding and to measure jet energies. The CAL is hermetic and consists of 5918 cells each read out by two photomultiplier tubes. Under test beam conditions the CAL has energy resolutions of $18\%/\sqrt{E\text{ (GeV)}}$ for electrons and $35\%/\sqrt{E\text{ (GeV)}}$ for hadrons. Jet energies were corrected for the energy lost in inactive material in front of the CAL which is typically about one radiation length (see Section 3.4). The effects of uranium noise were minimized by discarding cells in the electromagnetic or hadronic sections if they had energy deposits of less than 60 MeV or 110 MeV, respectively. The luminosity was measured from the rate of the bremsstrahlung process $e^+p \rightarrow e^+p\gamma$. A three-level trigger was used to select events online [8, 9].

3 Analysis

3.1 Offline Cleaning Cuts

To reject residual beam-gas and cosmic ray backgrounds, tighter cuts using the final z -vertex position, other tracking information and timing information are applied offline. Neutral current deep inelastic scattering (DIS) events with an identified scattered positron candidate in the CAL are removed from the sample as described in detail elsewhere [5, 9]. Charged current DIS events are rejected by a cut on the missing transverse momentum measured in the CAL. Finally, a restriction is made on the range of y , the fraction of the positron's energy carried by the incoming photon. The requirement, $0.15 < y_{\text{JB}} < 0.65$ is made where y_{JB} is an estimator of y which is determined from the CAL energy deposits according to the Jacquet-Blondel method [10]. This requirement corresponds to accepting events in the range $0.2 < y < 0.8$. These cuts restrict photon virtualities to less than about 1 GeV^2 with a median of around 10^{-3} GeV^2 .

3.2 Jet Finding

Jets are found using the KTCLUS [11] finder in the inclusive mode [12]. This is a clustering algorithm which combines objects with small relative transverse energy into jets. It is invariant under Lorentz boosts along the beam axis and is ideal for the study of multijet processes since it suffers from no ambiguities due to overlapping jets. Once the jets are determined, their transverse energy, pseudorapidity and azimuth are calculated according to the Snowmass convention [13]; $E_T^{\text{jet}} = \sum_i E_{T_i}$, $\eta^{\text{jet}} = (1/E_T^{\text{jet}}) \sum_i E_{T_i} \eta_i$ and

$\varphi^{\text{jet}} = (1/E_T^{\text{jet}}) \sum_i E_{T_i} \varphi_i$, where the sum runs over all objects assigned to the jet. The energies and three-vectors of the jets are then determined from the E_T^{jet} , η^{jet} and φ^{jet} . The objects input to the jet algorithm may be hadrons in a simulated hadronic final state, the final state partons of a pQCD calculation, or energy deposits in the detector. In the following, a jet quantity constructed from CAL cells with no energy correction has the superscript ‘‘CAL’’ while a jet quantity constructed from CAL cells and then subjected to a correction for energy loss in inactive material has the superscript ‘‘COR’’. There is no additional superscript for quantities referring to jets of final state partons or hadrons.

3.3 Monte Carlo Event Simulation

The response of the detector to jets and the acceptance and smearing of the measured distributions are determined using samples of events generated from Monte Carlo (MC) simulations. We have used the programs PYTHIA 5.7 [14] and HERWIG 5.9 [15] which implement the leading order matrix elements followed by parton showers. In these simulations multijet events can originate through this parton shower mechanism. Colour coherence in the parton shower is treated differently in the two models. In PYTHIA, parton showers are evolved in the squared mass of the branching parton with colour coherence effects implemented as a restriction on the opening angle of the radiation. In contrast, in HERWIG a parton shower evolution variable is chosen which automatically limits the branching to an angular ordered region. For both models, leading order direct and resolved processes are generated separately and combined according to the ratio of their generated cross sections. For the uncorrected distributions presented in this section the minimum transverse momentum of the partonic hard scatter (\hat{p}_T^{min}) was set to 4 GeV. In Section 4, corrected cross sections are presented and compared with the predictions from HERWIG and PYTHIA with $\hat{p}_T^{\text{min}} = 8$ GeV (our conclusions are insensitive to this parameter). The photon parton densities used were GRV LO [16] and the proton parton densities were CTEQ4 LO [17]. In the HERWIG simulation of the resolved processes, multiparton interactions have been included (these are not important in this kinematic regime, as discussed in Section 4).

The quality of these simulations is illustrated in Fig. 2 which shows the transverse energy flow around the jet axes. In this comparison the events have two jets with $E_T^{\text{jet CAL}} > 5$ GeV and a third jet with $E_T^{\text{jet CAL}} > 4$ GeV and jet pseudorapidities $|\eta^{\text{jet CAL}}| < 2.4$. The additional requirements on the CM quantities, $M_{3J}^{\text{CAL}} > 42$ GeV, $|\cos \vartheta_3|^{\text{CAL}} < 0.8$ and $X_3^{\text{CAL}} < 0.95$, have also been applied. These conditions represent those on the selected events (described in Section 3.5) to a good approximation. The jets have a narrow core with little transverse energy in the pedestal, except for the lowest $E_T^{\text{jet CAL}}$ jet where significant contribution to the ‘‘pedestal’’ from the other two jets in the event would be expected. In the $\Delta\varphi$ profiles of the two highest $E_T^{\text{jet CAL}}$ jets, the peaks near $\pm\pi$ indicate that these are roughly back-to-back. The PYTHIA and HERWIG event samples were passed through a detailed simulation of the ZEUS detector and the same selection criteria as for the data were applied. The MC samples provide a reasonable description of the energy flow in these three-jet events. HERWIG generates somewhat too little transverse energy in regions far from the jet core in φ for the lowest transverse energy jet, while PYTHIA slightly overestimates the transverse energy in the core of this jet. These models are also able to reproduce satisfactorily the

y_{JB} distribution for the three-jet events, the lab-frame $E_T^{\text{jet CAL}}$ and $\eta^{\text{jet CAL}}$ distributions as well as the transverse and longitudinal components of the boost from the lab-frame to the CM-frame (not shown).

3.4 Jet Energy Corrections

Jets of hadrons lose about 15% of their transverse energy when passing through inactive material before impinging on the CAL. This energy loss has been corrected using the MC samples [9, 18]. The KTCLUS algorithm was applied to the hadronic final state and from comparison of these hadron jets with the CAL jets obtained after the detector simulation, correction factors were determined as a function of $E_T^{\text{jet CAL}}$ and $\eta^{\text{jet CAL}}$. After applying these corrections the average shift in E_T^{jet} within the MC simulation is less than 2% and the E_T^{jet} resolution is 14%. This may be compared with the global jet energy scale uncertainty of $\pm 5\%$ [9]. The correction also reduces the shift in the reconstruction of M_{3J} from 16% to less than 1%. After these corrections for jet energy loss the average resolutions are 8% in M_{3J} , 0.03 units in X_3 , 0.05 units in X_4 , 0.03 units in $\cos \vartheta_3$ and 0.1 radians in ψ_3 and the distributions are well centred on their expected values.

3.5 Event Selection

After the jet energy correction the events are required to have at least two jets with $E_T^{\text{jet COR}} > 6$ GeV, a third jet with $E_T^{\text{jet COR}} > 5$ GeV and jet pseudorapidities in the range $|\eta^{\text{jet COR}}| < 2.4$. The requirement of high transverse energy for the jets ensures that the process should be calculable within pQCD. However, it introduces a bias in the angular distributions by excluding jets that are produced close to the beam-line. We make the additional requirements $M_{3J}^{\text{COR}} > 50$ GeV, $|\cos \vartheta_3|^{\text{COR}} < 0.8$ and $X_3^{\text{COR}} < 0.95$ to minimize such a bias. After these cuts the mean transverse energy of the highest, second-highest and third-highest transverse energy jet is about 20 GeV, 15 GeV and 10 GeV. From 16 pb^{-1} of data, 2821 events are selected. Around 15% of these have a fourth jet with $E_T^{\text{jet COR}} > 5$ GeV, in agreement with the prediction of the parton shower models. Backgrounds from beam gas and cosmic ray events, determined from unpaired bunch crossings, are negligible. The DIS contamination, determined using Monte Carlo techniques, is around 1% and neglected.

3.6 Acceptance Correction

The MC samples have been used to correct the data for the inefficiencies of the trigger and the offline selection cuts and for migrations caused by detector effects. The correction factors are calculated as the ratio $N_{\text{true}}/N_{\text{rec}}$ in each measured bin where N_{true} is the number of events generated in the bin and N_{rec} is the number of events reconstructed in the bin after detector smearing and all experimental cuts. The final bin-by-bin correction factors lie between about 0.7 and 1.3, the dominant effect arising from migrations across the M_{3J} threshold. The cross sections were determined using the corrections obtained with PYTHIA.

3.7 Systematic Uncertainties

A detailed study of the sources contributing to the systematic uncertainties of the measurements was performed [19]. Only the significant sources are listed here.

- The acceptance correction was performed using HERWIG instead of PYTHIA. The uncertainties associated with the model are typically around 20% and this forms the dominant uncertainty on the area-normalized distributions.
- The absolute energy scale of the detector response to jets with $E_T^{\text{jet}} > 5$ GeV is known to $\pm 5\%$ [9]. This leads to an uncertainty of 15 to 20% on the cross section. This is the dominant systematic uncertainty on the normalization of the cross section but as this uncertainty is highly correlated between bins it has a negligible effect on the area-normalized distributions.
- The results were recalculated allowing for fluctuations from outside the selected kinematic region by relaxing each of the cut parameters by 1σ of the resolution. This effect is typically 5%.

The systematic uncertainties have been added in quadrature to the statistical errors and this is shown as the outer error bars in the figures, with the exception of the absolute jet energy scale uncertainty which is shown as a shaded band for the cross sections. An overall normalization uncertainty of 1.5% from the luminosity determination has not been included.

4 Results and Discussion

The three-jet inclusive cross section is presented for events having at least two jets with $E_T^{\text{jet}} > 6$ GeV and a third jet with $E_T^{\text{jet}} > 5$ GeV where the jets satisfy $|\eta^{\text{jet}}| < 2.4$. This cross section refers to jets in the hadronic final state. To minimize the effects of these jet cuts on the distributions of physical interest, the requirements $M_{3J} > 50$ GeV, $|\cos \vartheta_3| < 0.8$ and $X_3 < 0.95$ have been imposed. The cross section is presented for photon-proton CM energies $W_{\gamma p}$ in the range $134 \text{ GeV} < W_{\gamma p} < 269 \text{ GeV}$ and the negative square of the invariant mass of the incoming photon extending to 1 GeV^2 . The cross section is $\sigma = 162 \pm 4(\text{stat.})_{-6}^{+16}(\text{sys.})_{-25}^{+32}(\text{energy scale}) \text{ pb}$.

A study using the PYTHIA MC indicates that hadronization effects are small ($\sim 5\%$), and flat in the distributions presented here [19]. The measurements are directly confronted with $\mathcal{O}(\alpha_s^2)$ pQCD calculations from two groups of authors [20, 21, 22]. The CTEQ4 LO [17] proton parton densities and the GRV LO [16] photon parton densities have been used in these calculations. The renormalization and factorization scales, μ , have been chosen to equal E_T^{max} , where E_T^{max} is the largest of the E_T^{jet} values of the three jets. α_s was calculated at one loop with $\Lambda_{\overline{\text{MS}}}^{(5)} = 181 \text{ MeV}$. As the calculations are leading order for three-jet production the normalization uncertainty due to the choice of μ is expected to be large. An uncertainty of a factor of two in the cross section for variation of μ between $E_T^{\text{max}}/2$ and $2E_T^{\text{max}}$ has been quoted [22].

The three-jet invariant mass distribution is shown in Fig. 3. The cross section falls approximately exponentially from the threshold value at 50 GeV to the highest measured value, around 150 GeV. The data are compared with the two $\mathcal{O}(\alpha_s^2)$ pQCD calculations.

These are in good agreement with the data, even though the calculations are leading order for this process. The M_{3J} distributions predicted by the parton shower models PYTHIA and HERWIG are also in agreement with the data in shape although the predicted cross sections are too low by 30-40%.

The distributions of the fraction of the available energy taken by the highest and second-highest energy jets are shown in Figs. 4 (a) and (b), respectively. Here the prediction for three jets uniformly distributed in the available phase space (i.e. with a constant matrix element) is also shown as the dotted curve. The parton shower models give a reasonable description of these energy sharing quantities. The pQCD calculations (overlapping) are in excellent agreement with these distributions. However, the similarity between the measured distributions and the three-body phase space prediction indicates that these distributions have little sensitivity to the pQCD matrix elements.

In Figs. 4 (c) and (d) the $\cos\vartheta_3$ and ψ_3 distributions are shown. These angular distributions are dramatically different from the distributions obtained from phase space, demonstrating that these quantities are sensitive to the pQCD matrix elements. The $\cos\vartheta_3$ distribution has forward and backward peaks, as expected. The $\mathcal{O}(\alpha\alpha_s^2)$ pQCD as well as the parton shower calculations, which take into account the dependence of this distribution on the spin of the exchanged quark or gluon, are in good agreement with the data. The jet algorithm and minimum E_T^{jet} requirements deplete the data near $\psi_3 \sim 0$ and π as indicated by the shape of the phase space curve in Fig. 4(d). With this taken into account, the data indicate a strong tendency for the three-jet plane to lie near the plane containing the beam and the highest energy jet. This effect is reproduced in the $\mathcal{O}(\alpha\alpha_s^2)$ matrix element calculations. It is interesting that the parton shower Monte Carlo programs PYTHIA and HERWIG are also able to provide a reasonable representation of the shape of the ψ_3 distribution.

Including a simulation of multiparton interactions in the parton shower programs has been found to improve significantly the description of low E_T^{jet} photoproduction [9]. In the present study the sensitivity to multiparton interactions has been investigated using both PYTHIA and HERWIG [19]. In neither case do secondary parton interactions cause a significant difference in the three-jet cross section in this kinematic regime, or in the angular distributions generated. It appears therefore that the third jet arises here from the parton shower and is not due to a second hard scatter.

Within the parton shower prescription, it is possible to separate the contributions of initial and final state parton showers. In Fig. 5(a) the three-jet cross section as a function of ψ_3 is shown and compared with the predictions of PYTHIA. The MC events have been separated into three samples; initial-state radiation only, final-state radiation only, and default PYTHIA which includes the interference of these two. The area-normalized distributions of ψ_3 are compared with these models in Fig. 5(b). Both the normalization and shape of these distributions indicate that the observed three-jet production occurs predominantly through initial state radiation with the final state radiation making a small contribution.

The QCD phenomenon of colour coherence is implemented in the PYTHIA parton shower model by prohibiting radiation into certain angular regions which are determined by the colour flow of the primary scatter. It is possible within this model to switch QCD colour coherence on and off. Figs. 5(c) and (d) again show the cross section and the area-normalized distribution with respect to ψ_3 compared with the HERWIG and PYTHIA predictions. The data lie above these predictions as previously mentioned,

however this discrepancy is not regarded as significant in view of the limited order of the calculation. The predictions do reproduce reasonably well the shape of the ψ_3 distribution. This is not the case if the simulation is done with colour coherence switched off. The incoherent PYTHIA prediction is relatively flat in ψ_3 . Coherence reduces the phase space available for large angle emissions as indicated by the drop in cross section around $\psi_3 \sim \pi/2$ for default PYTHIA. Colour coherence in the parton shower is needed to describe the shape of this distribution. QCD colour coherence seems to be a stronger effect in HERWIG than in PYTHIA however the present data are not precise enough to discriminate between these two simulations.

5 Summary

The inclusive cross section for the photoproduction of three jets has been measured by the ZEUS collaboration at HERA. $\mathcal{O}(\alpha\alpha_s^2)$ pQCD calculations are able to describe the cross section $d\sigma/dM_{3J}$, while parton shower models underestimate the cross section but are consistent in shape with the M_{3J} distribution. The angular distributions of the three jets are inconsistent with a uniform population of the available phase space but are well described by both fixed-order pQCD calculations and parton shower Monte Carlo models. Simulation of multiparton interactions does not help to describe the data in this kinematic regime. Within the parton shower model the three-jet events are found to occur predominantly due to initial state radiation, and the fundamental QCD phenomenon of colour coherence is seen to have an important effect on the angular distribution of the third jet.

Acknowledgements

The strong support and encouragement of the DESY Directorate have been invaluable, and we are much indebted to the HERA machine group for their inventiveness and diligent efforts. The design, construction and installation of the ZEUS detector have been made possible by the ingenuity and dedicated efforts of many people from inside DESY and from the home institutes who are not listed as authors. Their contributions are acknowledged with great appreciation. We warmly thank B. Harris, M. Klasen and J. Owens for providing their theoretical calculations.

References

- [1] UA2 Collab., J.A. Appel et al., *Z. Phys. C* **30** (1986) 341.
- [2] D0 Collab., S. Abachi et al., *Phys. Rev. D* **53** (1996) 6000.
- [3] CDF Collab., F. Abe. et al., *Phys. Rev. D* **54** (1996) 4221.
- [4] ZEUS Collab., M. Derrick et al., *Phys. Lett. B* **354** (1995) 163.
- [5] ZEUS Collab., M. Derrick et al., *Phys. Lett. B* **384** (1996) 401.
- [6] S. Geer and T. Asakawa, *Phys. Rev. D* **53** (1996) 4793.

- [7] ZEUS Collab., M. Derrick et al., *Phys. Lett. B* **293** (1992) 465.
- [8] The ZEUS Detector, Status Report 1993, DESY 1993.
- [9] ZEUS Collab., J. Breitweg et al., *Eur. Phys. J. C* **1** (1998) 109.
- [10] F. Jacquet and A. Blondel, in Proceedings of the Study for an *ep* Facility for Europe, ed. U. Amaldi, (DESY 79/48 1979), 391.
- [11] S. Catani, Yu.L. Dokshitzer, M. H. Seymour and B. R. Webber, *Nucl. Phys. B* **406** (1993) 187.
- [12] S. D. Ellis and D. E. Soper, *Phys. Rev. D* **48** (1993) 3160.
- [13] J. Huth et al., in Proceedings of the DPF 1990 Summer Study on High Energy Physics, Snowmass, Colorado, ed. E. L. Berger, (World Scientific, 1992), 134.
- [14] H.-U. Bengtsson and T. Sjöstrand, *Comp. Phys. Comm.* **46** (1987) 43.
- [15] G. Marchesini et al., *Comp. Phys. Comm.* **67** (1992) 465.
- [16] M. Glück, E. Reya and A. Vogt, *Phys. Rev. D* **46** (1992) 1973.
- [17] CTEQ Collab., H. L. Lai et al., *Phys. Rev. D* **55** (1997) 1280.
- [18] ZEUS Collab., J. Breitweg et al., *Eur. Phys. J. C* **4** (1998) 591.
- [19] E. Strickland, Ph.D. Thesis, University of Glasgow (1998).
- [20] B.W. Harris and J.F. Owens, *Phys. Rev. D* **56** (1997) 4007 and *private communication*.
- [21] M. Klasen, T. Kleinwort and G. Kramer, *Z. Phys.-e C* **1** (1998) 1, hep-ph/9712256.
- [22] M. Klasen, hep-ph/9808223.

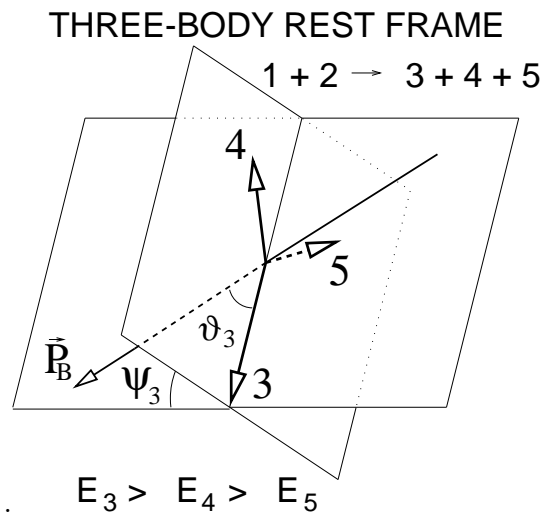


Figure 1: Illustration of the angles ϑ_3 and ψ_3 for a particular three-jet configuration. The beam direction is indicated by \vec{p}_B .

ZEUS 1995 – 1996

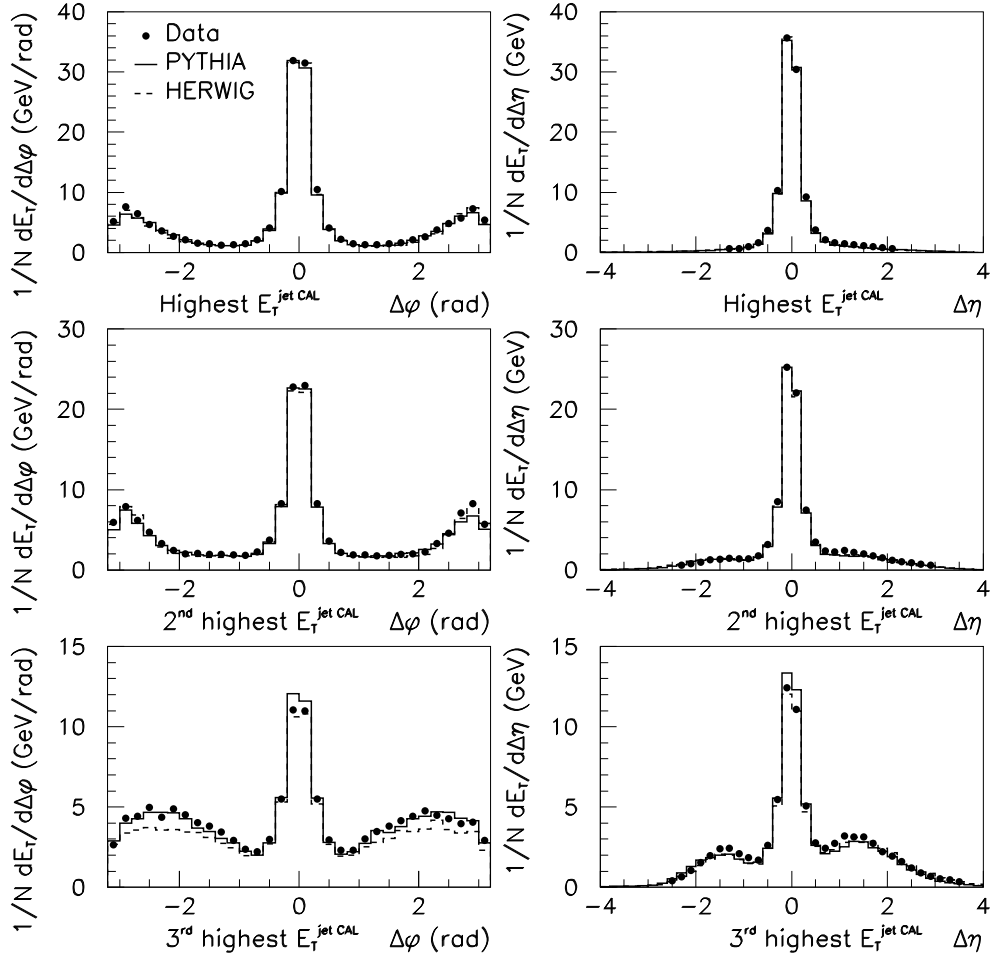


Figure 2: Uncorrected transverse energy flow with respect to the jet axis in the laboratory frame for three-jet events in order of $E_T^{\text{jet CAL}}$. On the left the uncorrected energy flow with respect to φ is shown for cells within one unit of η of the jet axis while on the right the profile with respect to η is shown for cells within one radian of φ of the jet axis. The data are shown as black dots while the PYTHIA and HERWIG predictions are shown by the solid and dashed histograms, respectively.

ZEUS 1995–1996

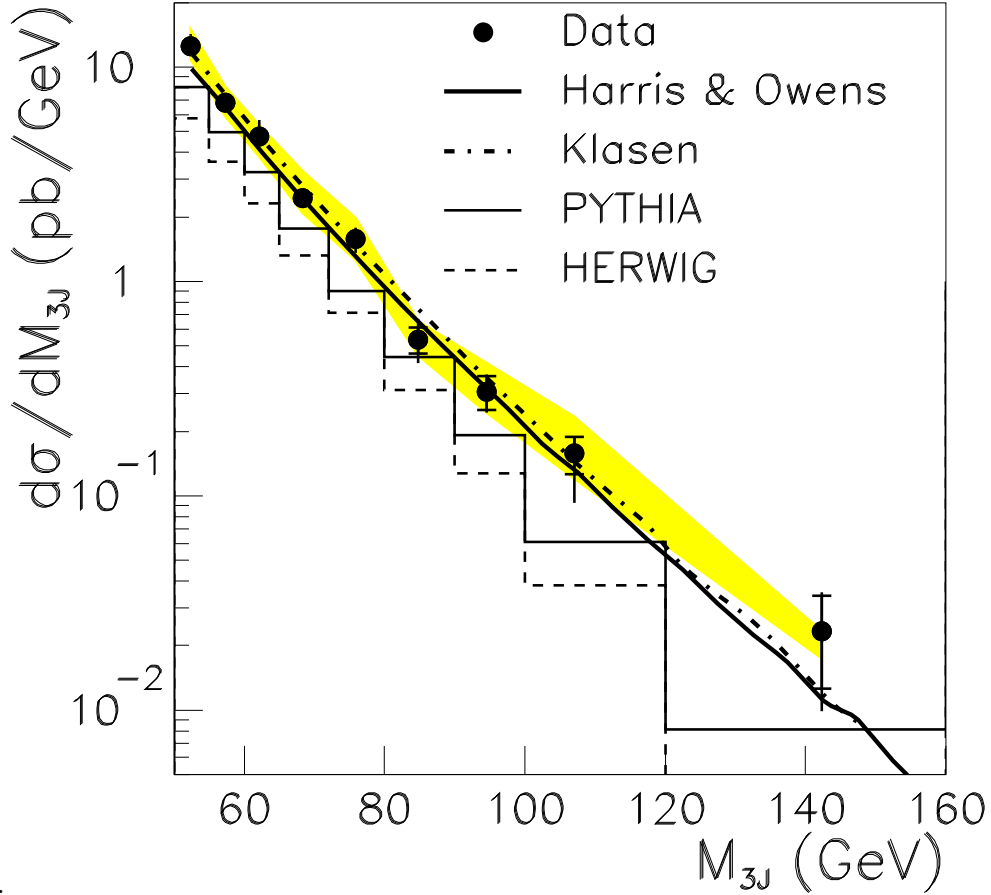


Figure 3: The measured three-jet cross section with respect to the three-jet invariant mass, $d\sigma/dM_{3J}$, is shown by the black dots where the inner error bar shows the statistical error and the outer error bar is the sum in quadrature of the statistical error and the systematic uncertainty. The jet energy-scale uncertainty, which is highly correlated between bins, is shown separately as the shaded band. $\mathcal{O}(\alpha_s^2)$ pQCD calculations by Harris & Owens and Klasen are shown by the thick solid and dot-dashed lines, respectively. The thin solid and dashed histograms show the predictions from two different parton shower models, PYTHIA and HERWIG.

ZEUS 1995–1996

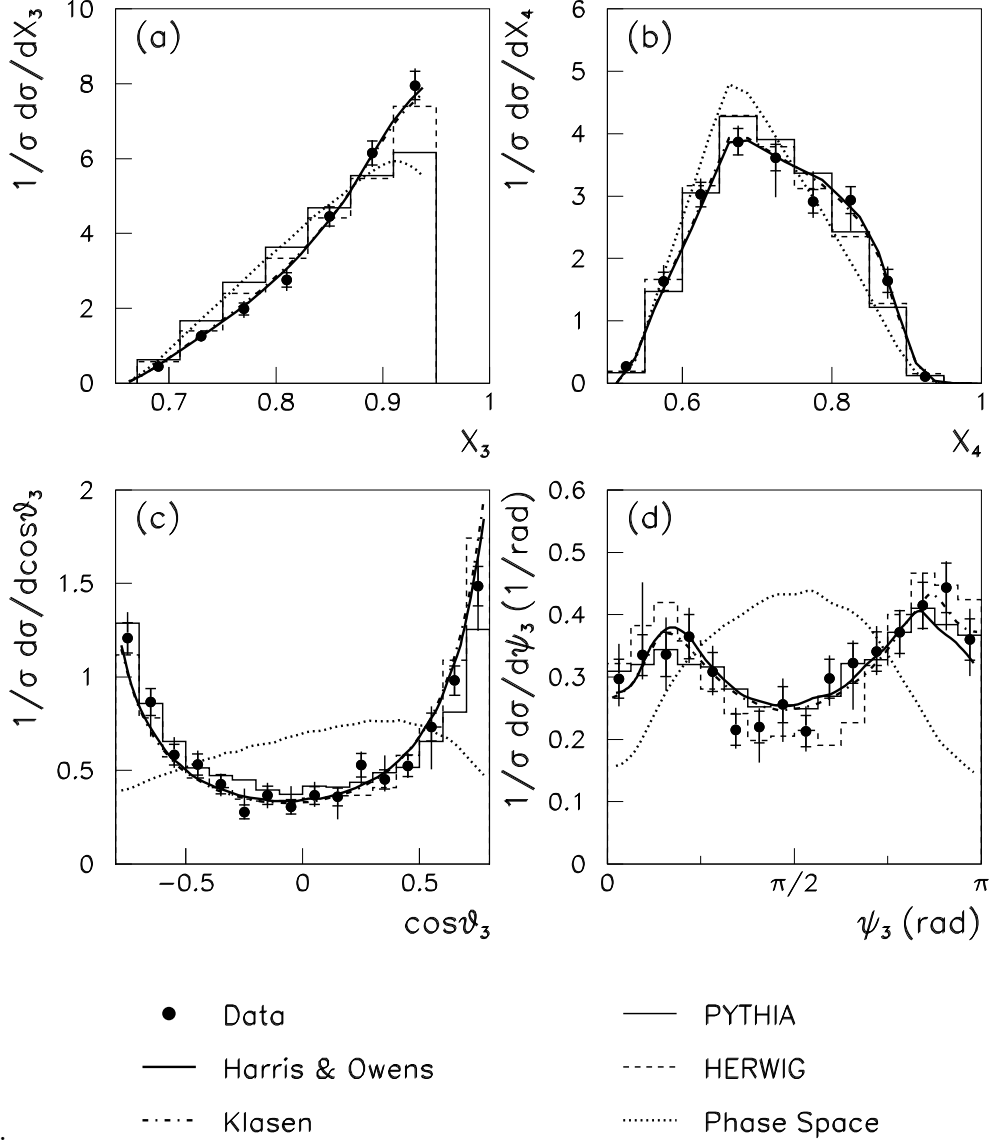


Figure 4: The distributions of the energy sharing quantities, X_3 and X_4 , are shown by the black dots in (a) and (b), respectively, and the distributions of the $\cos\vartheta_3$ and ψ_3 are shown in (c) and (d). Inner error bars show the statistical error and the outer error bars show the quadratic sum of this with the systematic uncertainty. The fixed-order pQCD predictions are shown by the thick solid and dot-dashed lines and the parton shower model predictions are shown by the thin solid and dashed histograms. The phase space distribution of three jets is indicated by the dotted line.

ZEUS 1995–1996

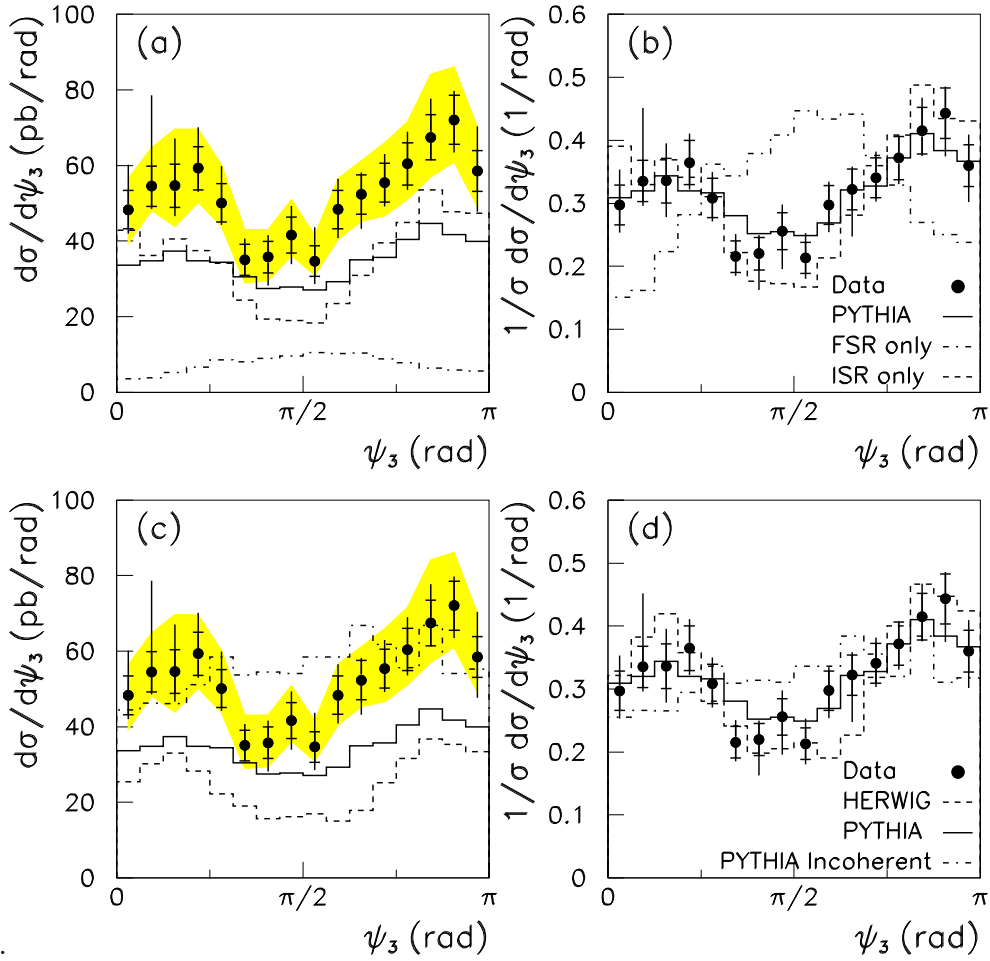


Figure 5: The measured cross section $d\sigma/d\psi_3$ is shown in (a) and (c) and the area-normalized distribution of ψ_3 is shown in (b) and (d). The error bars are as described previously with the correlated systematic uncertainty due to the jet energy-scale shown as the shaded band in (a) and (c). The solid histogram shows the default PYTHIA prediction. In (a) and (b) the dashed and dot-dashed histograms show the predictions from PYTHIA with final state radiation switched off and with initial state radiation switched off. In (c) and (d) the dashed and dot-dashed histograms show the predictions of HERWIG and of PYTHIA with colour coherence switched off.